

Ral Overactivation in Malignant Peripheral Nerve Sheath Tumors[∇]

Vidya Bodempudi,² Farnaz Yamoutpoor,² Weihong Pan,² Arkadiusz Z. Dudek,² Tuba Esfandyari,¹ Mark Piedra,³ Dusica Babovick-Vuksanovic,³ Richard A. Woo,⁴ Victor F. Mautner,⁵ Lan Kluwe,⁵ D. Wade Clapp,⁶ George H. DeVries,⁷ Stacey L. Thomas,⁷ Andreas Kurtz,⁸ Luis F. Parada,⁹ and Faris Farassati^{1*}

Molecular Medicine Laboratory, University of Kansas School of Medicine, Department of Medicine, Kansas City, Kansas¹; University of Minnesota, Minneapolis, Minnesota²; Mayo Clinic, Rochester, Minnesota³; Southern Illinois University, Springfield, Illinois⁴; University Hospital Eppendorf, Hamburg, Germany⁵; University of Indiana School of Medicine, Indianapolis, Indiana⁶; Research Service, Edward Hines, Jr., V.A. Hospital, Hines, Illinois⁷; Massachusetts General Hospital, Charlestown, Massachusetts⁸; and University of Texas Southwestern Medical Center, Dallas, Texas⁹

Received 21 July 2008/Returned for modification 8 September 2008/Accepted 30 March 2009

Ras leads an important signaling pathway that is deregulated in neurofibromatosis type 1 and malignant peripheral nerve sheath tumor (MPNST). In this study, we show that overactivation of Ras and many of its downstream effectors occurred in only a fraction of MPNST cell lines. RalA, however, was overactivated in all MPNST cells and tumor samples compared to nontransformed Schwann cells. Silencing Ral or inhibiting it with a dominant-negative Ral (Ral S28N) caused a significant reduction in proliferation, invasiveness, and in vivo tumorigenicity of MPNST cells. Silencing Ral also reduced the expression of epithelial mesenchymal transition markers. Expression of the NF1-GTPase-related domain (NF1-GRD) diminished the levels of Ral activation, implicating a role for neurofibromin in regulating RalA activation. NF1-GRD treatment caused a significant decrease in proliferation, invasiveness, and cell cycle progression, but cell death increased. We propose Ral overactivation as a novel cell signaling abnormality in MPNST that leads to important biological outcomes with translational ramifications.

The Ras family of guanine-nucleotide bound proteins exerts a fundamental role in cell biology and constitutes an important area of cancer research due to its significant involvement in the development and progression of malignancies (8, 10, 17, 18, 32). Ras-like (Ral) proteins are crucial members of this family and have been shown to play a pivotal role in human tumors (7, 28, 41, 66, 70). Because Ral guanine nucleotide exchange factors (Ral-GEFs) are direct effectors of Ras, the Ral signaling pathway has been traditionally considered a Ras-effector pathway. Activation of Ras (in resemblance to Ral) is regulated by two classes of proteins: Ras-GEFs (e.g., SOS) and Ras-GTPase activating proteins (Ras-GAPs such as neurofibromin). The latter induces hydrolysis of Ras from the active (GTP) form to the inactive (GDP) form (13). Ral-GEFs include two main groups: the proteins that are stimulated by Ras because of their carboxy-terminal Ras binding domain (RalGDS, RGL1, and RGL2) and the proteins that are activated by substrates of PI3K through a pleckstrin homology domain on their C-terminal (RALGPS1 and RALGPS2) (19). Although highly similar to Ras, Ral proteins (RalA and RalB) involve a series of distinctly different effectors that influence gene expression and translation through interaction with ZO-1-associated nucleic acid binding protein (ZONAB) and RalA binding protein 1 (RalBP1) (11, 23, 33). RalB directly interacts with the SEC5 subunit of exocyst to facilitate the host defense response (48, 58).

In addition to overactivation of GEFs, inactivation of GAPs is another mechanism for overactivation of GTP-bound proteins. The lack of neurofibromin (encoded by *NF1* on human chromosome 17q11.2), a Ras-GAP protein, is the main molecular event in neurofibromatosis type 1 (NF-1), an autosomal-dominant human genetic disease occurring in approximately 1 in 2,500 to 3,500 births (22, 27, 42). One of the main tumor-causing effects of inactivating mutations in the tumor suppressor *NF1* gene is postulated to be the subsequent activation of Ras (3, 29, 53, 57, 69). With two main functional domains, SEC14 and Ras-GAP, neurofibromin is best known for its Ras-GAP function. Although the yeast SEC14p is shown to be involved in regulating intracellular proteins and lipid trafficking, the function of its homologous domain in neurofibromin is unknown (49, 62). Although neurofibromas are the most common tumors in NF-1, 10% of patients with plexiform develop malignant peripheral nerve sheath tumors (MPNSTs), which are typically high grade and often fatal (21, 34, 65).

The molecular events involved in the malignant transformation of benign neurofibromas to MPNST are poorly defined. Usually arising in the third through sixth decades of life, these tumors are composed of tightly packed hyperchromatic spindle-shaped cells with frequent mitotic figures. Inactivation of both copies of the *NF1* gene has been demonstrated in benign human neurofibromas and shown to cause tumors in murine models (56). Loss of heterozygosity of *NF1* and *p53* has frequently been observed in human MPNST (35, 47, 54). Recombinant mouse strains (NP mice), which harbor inactivated *Nf1* and *p53* alleles (*cis-Nf1*^{+/-}:*p53*^{+/-}), demonstrate the cumulative effects of loss of both *Nf1* and *p53* genes in the etiology of MPNST (14, 68).

In the present study, we show that while both Ras activation

* Corresponding author. Mailing address: KUMC-Molecular Medicine Laboratory, 1000 Hixon, Mail Stop 4037, 3901 Rainbow Blvd., Kansas City, KS 66160. Phone: (913) 945-6823. Fax: (913) 945-6923. E-mail: ffarassati@kumc.edu.

[∇] Published ahead of print on 4 May 2009.

and activation of a series of its downstream effector pathways are observed in a fraction of MPNST cells, RalA is activated globally in all studied mouse and human MPNST cells and tumor samples. Our results also explain the involvement of this signaling molecule in a series of key biological functions of MPNST cells, as shown in a variety of in vitro assays and an in vivo model of MPNST. Such information may play a role in designing novel therapies for treatment of MPNST or other tumors with overactivation of the Ral pathway.

MATERIALS AND METHODS

Cell culture, viruses, and plasmids. Mouse MPNST cells (6IE4, 37-3-18, 35-1-2, 38-2-18, and 32-5-24-12 cells) were originally isolated from different mouse MPNSTs and were confirmed for lack of *Nf1* and *p53* expression (68). Mouse Schwann cells (SW10) were purchased from the American Type Culture Collection (ATCC number CRL-2766), and human Schwann cells were purchased from ScienCell Research Laboratories. Human 94.3 and 94.3GRD cells, NF1-GRD and control retroviruses, and packaging GP-293 cells were from the laboratory of G. H. DeVries (59). NF1-GRD and control plasmids were from the laboratory of D. W. Clapp (59). RalA-S28N containing plasmid was purchased from Upstate and has been described previously (2). S805 cells were from the laboratory of V. F. Mautner (45). All cells were maintained in Dulbecco modified Eagle medium with 10% fetal bovine serum supplemented with antibiotics. Specialty media were provided for human Schwann cells by ScienCell Research Laboratories.

Affinity pulldown assays for Ras and Ral. Ras and Ral activation assays (Upstate) were performed in accordance with the manufacturer's instructions. Briefly, cells grown in 10-cm tissue culture dishes were lysed at 75 to 80% confluence. After determination of the protein concentration, 7.5 μ g of Ral assay reagent (Ral BP1, agarose) or Ras assay reagent (Raf-1 RBD, agarose) was added to 200 μ g of total cell protein in 200 μ l of Mg²⁺ lysis buffer. After a period of rocking at 4°C, the activated GTP forms of Ras/Ral bound to the agarose beads were collected by centrifugation, washed, boiled in 2 \times Laemmli reducing sample buffer (Bio-Rad), and loaded onto a 10% sodium dodecyl sulfate-polyacrylamide gel electrophoresis (SDS-PAGE) gel (Bio-Rad). The proteins were transferred to a nitrocellulose membrane, blocked with Tris-buffered saline-0.2% Tween-5% milk, and incubated with anti-RalA or anti-Ras antibody (1:1,000). The membranes were then washed with Tris-buffered saline-Tween for 10 min each and then incubated with sheep anti-mouse horseradish peroxidase-conjugated immunoglobulin G (Amersham) at 1:2,000. Bands were detected by using LumiGLO chemiluminescent reagent peroxidase (Cell Signaling).

Nonradioactive Ras downstream kinase assays. Nonradioactive Ras effector assays (Cell Signaling) were performed in accordance with the manufacturer's instructions. Briefly, cells grown in 10-cm tissue culture dishes were lysed at 75 to 80% confluence with 300 μ l of cell lysis buffer. Immobilized antibody-bead slurry capable of binding to the phosphorylated forms of extracellular signal-regulated kinase (ERK), JUN, AKT, and p38 kinase were then added to 200 μ g of total cell protein in 200 μ l of cell lysis buffer. The mixture was incubated with gentle rocking overnight at 4°C and then collected, washed, and introduced to an in vitro kinase reaction in the presence of ATP and a special buffer. The levels of phosphorylated ELK, JUN, ATF2, and AKT were then assayed by Western blotting with antibodies directed against the phosphorylated forms of these proteins.

Small interfering RNA (siRNA) preparation. Upon arrival, the double-stranded oligonucleotide was resuspended in the related buffer and then incubated in 95°C for 1 min, followed by 37°C for 1 h according to the manufacturer's (Qiagen) instructions.

Electroporation. The mouse anti-Ral siRNA (Ral-siRNA) (5'-AAGCATGC TGTTAGGAATGTA) and negative control siRNA (5'-UUCUCCGAACGUG UCACGUdTdT) (Qiagen and Santa Cruz, respectively) are introduced to the cells by electroporation. This method is considered transient since the concentration of siRNA in the target cells eventually drops to nonefficient levels. A total of 1×10^6 to 2×10^6 cells is resuspended in 270 μ l of Opti-MEM and mixed with 30 μ l of 20 μ M siRNA stock solution, generating a final concentration of 2 μ M siRNA. This cocktail was then transferred to an electroporation cuvette (Bio-Rad) while being kept on ice and electroporated at 300 mV for one 10-s pulse. The cells in the cuvette were then incubated at 37°C for 2 h. The cells were then washed, resuspended in 2 ml of their growth media, and transferred to a flow cytometry facility for sorting. SDS-PAGE, and Western blot analysis.

Different cells were lysed with a single detergent lysis buffer (50 mM Tris [pH

8.0], 150 mM NaCl, 0.02% sodium azide, 100 μ g of phenylmethylsulfonyl fluoride/ml, 1 μ g of aprotinin/ml, 1% Triton X-100) and normalized for the amount of total protein. The cells were then subjected to SDS-PAGE using a Bio-Rad Mini-Cell Protein-II system (using precast 10% or 8 to 16% gradient discontinuous gels) and then subjected to electroblotting onto nitrocellulose paper. The membrane was then washed, incubated with the primary antibodies against epithelial mesenchymal transition (EMT) markers (Cell Signaling) or neurofibromin (Santa Cruz Biotechnology), and incubated with horseradish peroxidase-conjugated secondary antibody against mouse or rabbit. After appropriate washing, the blots were exposed to Lumigel detection solution and subjected to autoradiography.

Cell invasion assay. In order to evaluate cell invasiveness, a commercial kit was used (BD Biosciences). Briefly, cells (50,000 control or test cells) were introduced into Matrigel-coated inserts fitting 24-well plates. As the cells penetrated the layer of Matrigel, the fraction of invaded cells was detected by staining them with crystal violet and quantifying them by spectroscopy. Invaded cells were fixed with 5% paraformaldehyde, stained with a 5% solution of crystal violet, and then photographed to obtain a visual representation of their density. The cells were then solubilized in a 3% detergent (NP-40) solution, and the absorbance was measured by spectrophotometry at 590 nm.

Cell proliferation assay. The cell proliferation assay was performed using a kit (Chemicon) according to the manufacturer's instructions. The assay is based on the cleavage of the tetrazolium salt WST-1 to formazan by cellular mitochondrial dehydrogenases. Expansion in the number of viable cells increases the overall activity of the mitochondrial dehydrogenases and in turn increases the amount of formazan dye formed. Briefly, 10^4 cells/well were seeded in a 96-well microplate in volume of 100 μ l/well. At different times, 10 μ l of WST-1/ECS solution was added to each well. The plates were incubated for 4 h in standard culture conditions. The plates were then shaken thoroughly for 1 min. The absorbance was measured at 480 nm.

s.c. model for in vivo tumorigenicity in SCID mice. siRNA transfected cells were injected subcutaneously (s.c.) in the flank of 10 5- to 6-week-old male Fox Chase SCID outbred mice (CrI:HA-Prkdc^{scid}; Charles River Laboratories). Control treated cells were injected into the right flank, and Ral-siRNA treated cells were injected into the left flank (5×10^5 cells/flank). Animals were checked for tumor development every other day, and the tumor size was measured by using a digital caliper. The tumor volume was determined with the following formula: tumor volume (mm³) = [length (mm)] \times [width (mm)]² \times ϕ .

Statistical analysis. Results are reported as means \pm the standard deviation. A Student *t* test was used to analyze statistical differences between groups. The α level was set at 0.05.

RESULTS

Constant overactivation of Ral versus variable activation of Ras and Ras effector pathways in MPNST cell lines. Ras-activation stimulates a variety of effector pathways including ERK (9), Jun amino-terminal kinase (JNK), p38 kinase, and phosphatidylinositol 3-kinase (PI3K), and Ral (18, 24, 25, 29, 30, 52) (Fig. 1A and B). We compared the activation of Ras, Ral, and other Ras downstream effector pathways in five mouse MPNST cell lines from distinct tumors (6IE4, 37-3-18, 35-1-2, 38-2-18, and 32-5-24-12) and a nontransformed mouse Schwann cell line (SW10). Although Ras and the ERK, JNK, p38K, and PI3K pathways were overactivated in 6IE4 and 37-3-18, their level of activation in the other three cell lines was not higher than SW10 cells (Fig. 1A). Ral levels, however, were consistently elevated in all MPNST cell lines in comparison to SW10 cells (Fig. 1B). Because the Ras-GAP function of neurofibromin is lost in these MPNST cell lines, it is important that only a fraction of MPNST cells show elevated levels of Ras while Ral remains overactive in all MPNST cell lines.

Ral silencing reduces cell viability of MPNST cells but not Schwann cells. In order to investigate further the involvement of Ral signaling in the growth of MPNST cells, we used siRNA to silence the expression of RalA in a specific manner. Treatment of MPNST cells (35-1-2) with Ral-siRNA caused a sig-

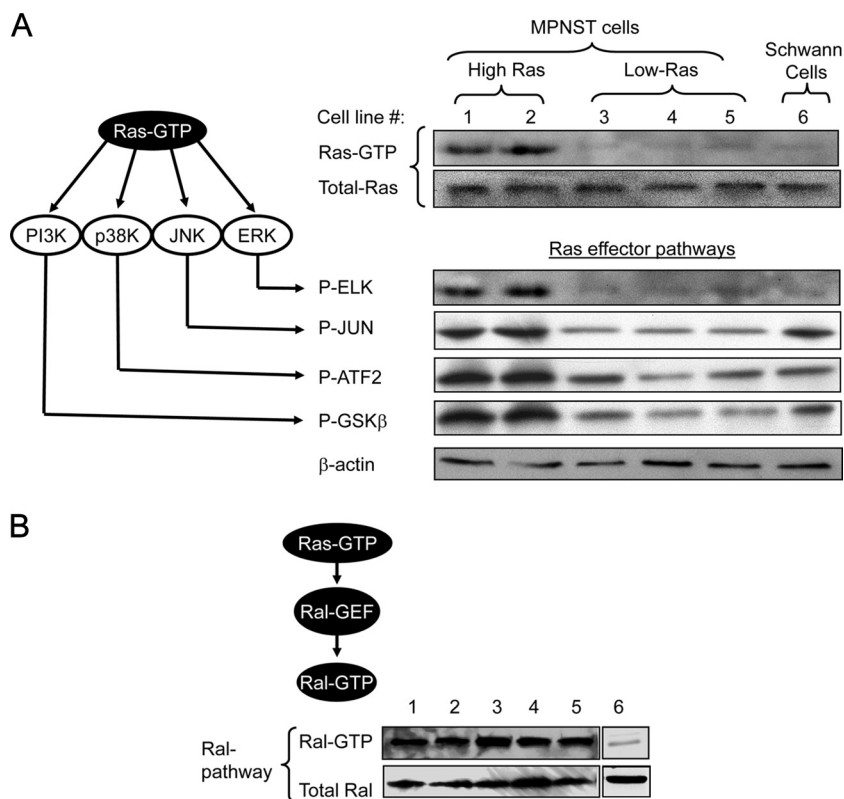


FIG. 1. Activation of Ras and Ral signaling pathways in mouse MPNST cells. (A) Ras signaling induces the activation of a series of effector pathways (left panel). The activity of Ras in different mouse MPNST cell lines and Schwann cells was detected by a Ras affinity pulldown assay for Ras-GTP. The right panel shows the amount of the activated form of Ras (Ras-GTP). The lower panel shows the amount of the total form of Ras. ERK pathway activation was evaluated by measuring the phosphorylation of ELK by immobilized phospho-ERK in an in vitro kinase assay. The activity of other Ras downstream effector pathways were investigated by similar pulldown assays coupled with in vitro kinase reactions for JUN, p38, and PI3K pathways. In each assay, an in vitro kinase reaction was performed to detect the capability of each effector in phosphorylating its specific substrate, which was in turn detected by blotting with a phospho-specific antibody. Cell lines are numbered in panel A as follows: 1, 6IE4; 2, 37-3-18; 3, 35-1-2; 4, 38-2-18; and 5, 32-5-24-12. Cell lines 6IE4 and 37-3-18 are referred to as High-Ras. Cell lines 35-1-2, 38-2-18, and 32-5-24-12 are referred to as Low-Ras. Activated levels of Ras (H-, K-, and N-Ras) and other effector pathways were determined under growth conditions in the presence of 10% fetal bovine serum. (B) Affinity pulldown assay for Ral-GTP was performed in lysates from different MPNST cell lines, as well as nontransformed mouse SW10 Schwann cells. The amount of total RalA was detected with a monoclonal antibody against this protein. Cell lines are numbered as in panel A. Activated levels of RalA were determined under growth conditions in the presence of 10% fetal bovine serum.

nificant reduction of Ral expression to $\sim 30\%$ of basal levels within 48 to 72 h (Fig. 2A). We observed no effects on the expression of β -actin as a control for specificity of Ral-siRNA. Ral-siRNA treatment also significantly decreased the proliferation rate of these cells at 48 to 72 h after exposure to siRNA in comparison to control-treated cells (Fig. 2B; $P < 0.001$). We plotted the growth rate of Ral-siRNA-treated samples as a percentage of mock-treated cells at each time point. Although we observed no significant difference for days 1 and 4, the proliferation rates of the Ral-siRNA-treated and control-treated cells were significantly different at days 2 and 3 (Fig. 2B). Interestingly, upon partial abrogation of Ral silencing at day 4, the proliferation rate of 35-1-2 cells returned to pre-siRNA treatment levels. The density of cell confluence at day 3 postelectroporation was also much lower for cells treated with Ral-siRNA (Fig. 2B, callout panels).

Ral silencing reduces invasiveness of MPNST cells and affects the expression pattern of EMT markers. Once we evaluated 35-1-2 cells for their invasiveness by migration through a

layer of Matrigel, we found a significant ($P < 0.002$) reduction in the invasiveness of these cells upon silencing Ral. Figure 2C shows the results of cell invasion assay upon Ral silencing at day 3 postelectroporation. The callout panels show the density of invaded cells stained with crystal violet at this time point.

To understand further the mechanism for such loss of invasiveness of MPNST cells, we evaluated the expression of a series of EMT markers under conditions in which Ral was silenced. As shown in Fig. 2D, the expression of transcription factors β -catenin and Snail was remarkably reduced while Slug, another transcription factor involved in EMT was not significantly changed. The process of "E- to N-cadherin switch," considered an important step in EMT in tumor cells, was also affected by Ral silencing, since the levels of N-cadherin were significantly decreased, while those of E-cadherin were not changed notably. Overall, the process of EMT appeared to be reversed by silencing Ral in MPNST cells.

Ral silencing in nonmalignant Schwann cells does not influence proliferation rate in a significant manner. To deter-

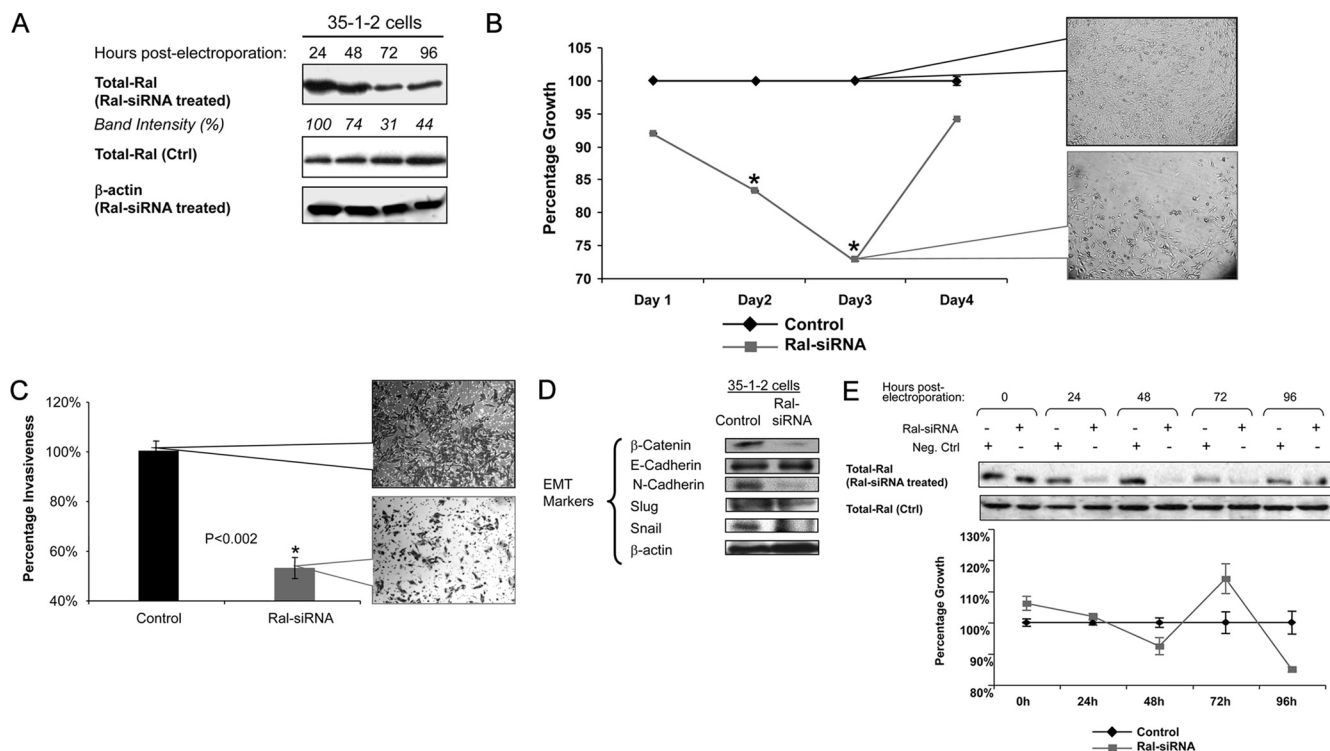


FIG. 2. Effects of Ral silencing on the biology of MPNST and Schwann cells. (A) Ral-siRNA (2 μ M final concentration) was introduced to 35-1-2 cells by electroporation followed by Western blotting for Ral expression. Lysates from Ral-siRNA-treated cells were blotted for expression of RalA at different times postelectroporation in order to verify silencing. Intensity is reported for each band. β -Actin was probed as a control for specificity of the Ral-siRNA against its target. Control-treated cell lysates were also blotted for expression of RalA. (B) A significant reduction in the growth rate of Ral-siRNA treated cells was seen on days 2 and 3 but not on days 1 or 4 compared to the proliferation rate of control-treated cells, which were considered as 100% at each time point. Callout panels provide visualization of cell confluence at day 3 after electroporation. Asterisks represent a significant difference between counterpart time points ($P < 0.001$). (C) A significant reduction in invasiveness of cells ($P < 0.002$) was observed upon silencing Ral in 35-1-2 cells. Cells were electroporated with Ral-siRNA as described in G and introduced into a cell invasiveness assay. Cells were photographed at 3 days postelectroporation. Invasiveness was assayed by measuring the absorbance of cells stained with crystal violet. Callout panels represent cell density at 3 days postelectroporation. (D) Expression of EMT markers was evaluated upon silencing Ral at 48 h postelectroporation with Ral-siRNA in 35-1-2 cells. (E) Ral-siRNA (2 μ M final concentration) was introduced into SW10 cells by electroporation, followed by Western blotting for Ral expression and an assay for cell proliferation. Lysates from Ral-siRNA-treated cells were blotted for expression of Ral at different times postelectroporation in order to evaluate silencing (upper panel). No significant changes in the growth rate of SW10 cells was seen compared to the proliferation rate of mock-treated cells (lower panel). The latter were plotted as 100% at each time point.

mine whether Ral silencing would influence the viability of nontransformed Schwann cells, we electroporated SW10 cells in the same manner as described above and evaluated their viability in comparison to control treated cells. As seen in Fig. 2E, silencing Ral did not induce any significant change in the viability of SW10 cells within 96 h after electroporation with Ral-siRNA. The silencing of Ral remained in effect up to 72 h postelectroporation with recruitment of Ral expression to levels close to those of the control at 96 h postelectroporation.

Inhibition of Ral activation by dominant-negative Ral reduces the viability and invasiveness of MPNST cells. Because inhibition of Ral expression by siRNA silencing reduced the growth rate of 35-1-2 MPNST cells, we decided to investigate whether suppression of Ral activation would also suppress the proliferation of MPNST cells. For this purpose, we used an alternative MPNST cell line, 37-3-18, and transfected these cells with a plasmid containing S28N, a dominant-negative version of Ral, and the fluorescent protein DsRed-express (pS28N-IRES-Dsred-express) or a control plasmid consisting

of the backbone void of S28N. At 72 h postelectroporation, the proliferation rate of 37-3-18 cells was reduced (Fig. 3A, $P < 0.05$) in conjunction with an $\sim 68\%$ reduction in Ral-GTP levels compared to control-treated cells (Fig. 3B). At this time point, the invasiveness of 37-3-18 cells was also reduced to 10% of the level of the control levels (Fig. 3C, $P < 0.05$).

Finally, we were interested to determine whether inhibition of geranyl-geranylation, a posttranslational modification highly required for Ral activation, would affect the proliferation of MPNST cells. In order to study this, we used geranyl-geranyl transferase inhibitor 2147 (GGTI-2147), a cell-permeable non-thiol peptidomimetic that acts as a potent and selective inhibitor of geranylgeranyl-transferase I (GGTase I) (6, 67). GGTI-2147 has been shown to block the geranyl-geranylation of Rap1A with a 50% inhibitory concentration that is >60 -fold lower than that required to disrupt the farnesylation of H-Ras (6, 67). Figure 3D shows that at a 250 nM concentration of this drug the proliferation rate of MPNST cells (37-3-18) is reduced in a significant manner (lower panel). Interestingly, at

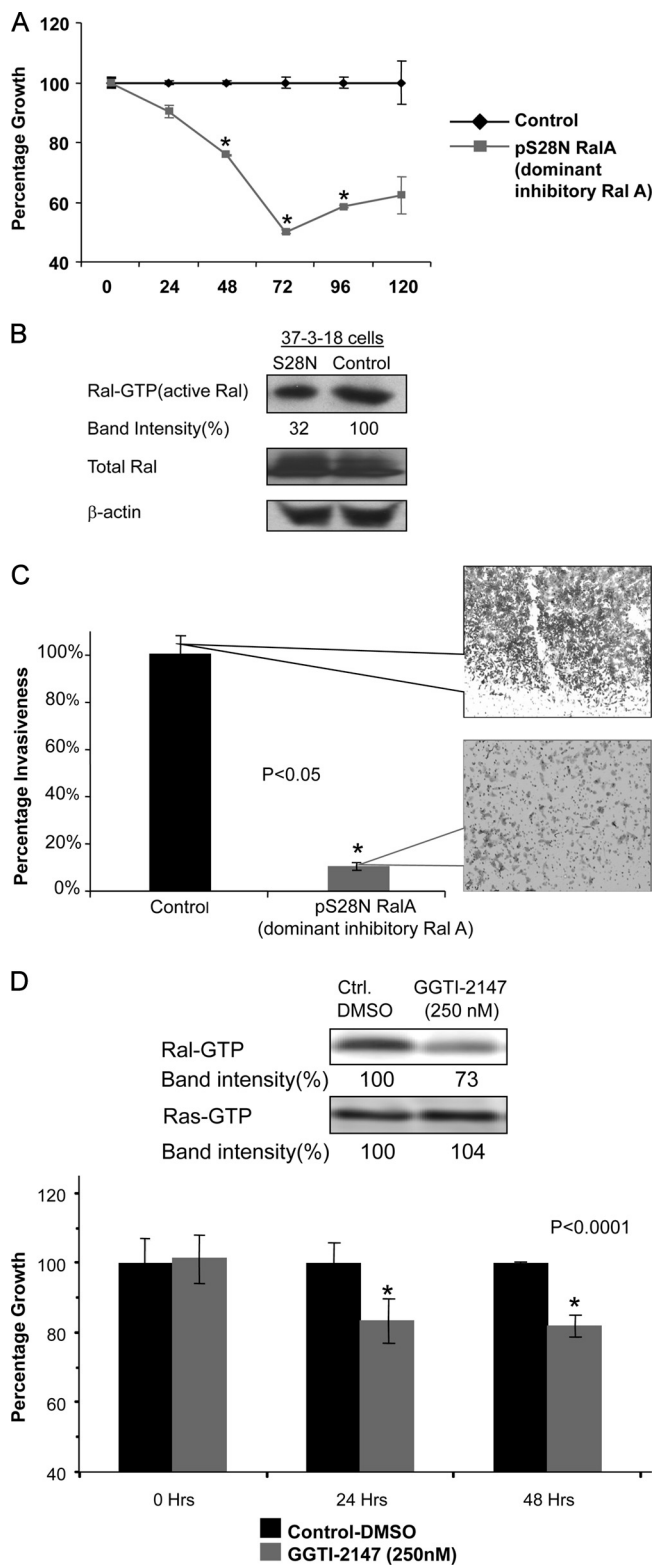


FIG. 3. Inhibition of Ral activation in mouse MPNST cells. (A) Mouse MPNST cells (37-3-18) were electroporated with a plasmid containing the dominant-negative version of Ral named S28N. At 72 h postelectroporation, the proliferation rate of these cells was reduced significantly upon reduction of Ral activity. (B) Treatment of 37-3-18 cells with the plasmid expressing S28N (dominant-negative Ral) resulted in the reduction of Ral-GTP at 72 h postelectroporation. The

such a concentration, while the level Ral-GTP was decreased, the Ras-GTP levels stayed unchanged (upper panel).

Ral activation in human MPNST is reduced by expression of NF1-GRD. Once our murine data demonstrated that Ral is critical to the proliferation and invasiveness of mouse MPNST cells, we extended these findings to human MPNST cells and tissues. To do this, we used two primary human MPNST cells from independent sources, namely, 94.3 and S805 cells and the derivatives of these cells, which were transfected with a retrovirus expressing NF1-GAP related domain (NF1-GRD). As seen in Fig. 4A, Ral activation in 94.3 cells is reduced to levels comparable to primary human nontransformed Schwann cells once NF1-GRD is expressed in these cells. The levels of Ral activation were also reduced to beneath detectable levels upon exposure of S805 cells to NF1-GRD virus. In addition, we detected Ral overactivation in lysates from three human MPNST samples (named HuMPNST-1, -2, and -3) compared to primary human Schwann cells (Fig. 4A, top right panel).

Although all human MPNST primary cells and tumor samples showed Ral overactivation (in comparison to nontransformed Schwann cells), we observed the overactivation of Ras prominently in S805 and HuMPNST-3 (Fig. 4A, lower panel).

Expression of NF1-GRD decreases proliferation and invasiveness of human MPNST cells. We next investigated whether reduction of Ral activation by expression of NF1-GRD would affect the biological characteristics of human MPNST cells. We observed that the proliferation rate of 94.3 cells was reduced after 48 h of infection with the NF1-GRD virus at a multiplicity of infection of 1 compared to the control virus (empty vector) (Fig. 4B). We also saw a significant reduction in the invasiveness of NF1-GRD-expressing MPNST cells after 48 h of exposure of 94.3 cells to NF1-GRD virus compared to the control virus (Fig. 4B, lower panel). A similar pattern was also observed (reduction in proliferation and invasiveness) for S805 cells exposed to NF1-GRD and control viruses (Fig. 4C). Notably, although S805 cells appear to be much more invasive than 94.3 cells in the control group, their invasiveness was significantly reduced upon exposure to NF1-GRD.

Expression of NF1-GRD alters cell cycle progression of human MPNST cells and increases the rate of cell death. We next investigated the effects of expression of NF1-GRD and a subsequent decrease in Ral activation on cell cycle progression of human MPNST cells. As shown in Fig. 5A and B, both 94.3 and S805 cells exposed to the NF1-GRD virus showed a decrease in the fraction of G₁ cells and an increase in the fraction of S and G₂ cells compared to cells exposed to the control virus ($P < 0.01$). The rate of cell death was increased more than 2.5-fold for both cell types under such conditions (Fig. 5C).

total amount of Ral as well as β -actin remained unchanged. (C) Invasiveness of 37-3-18 cells at 72 h after electroporation with a plasmid expressing S28N. Callout panels provide a visualization of the density of invaded cells at this time point. (D) GGTI-2147 has been shown to block the geranyl geranylation, a posttranslational modification involved in Ral activation. Although the level Ral-GTP was decreased, Ras-GTP levels stayed relatively unchanged (upper panel). At a 250 nM concentration of this drug the proliferation rate of MPNST cells is reduced in a significant manner (lower panel).

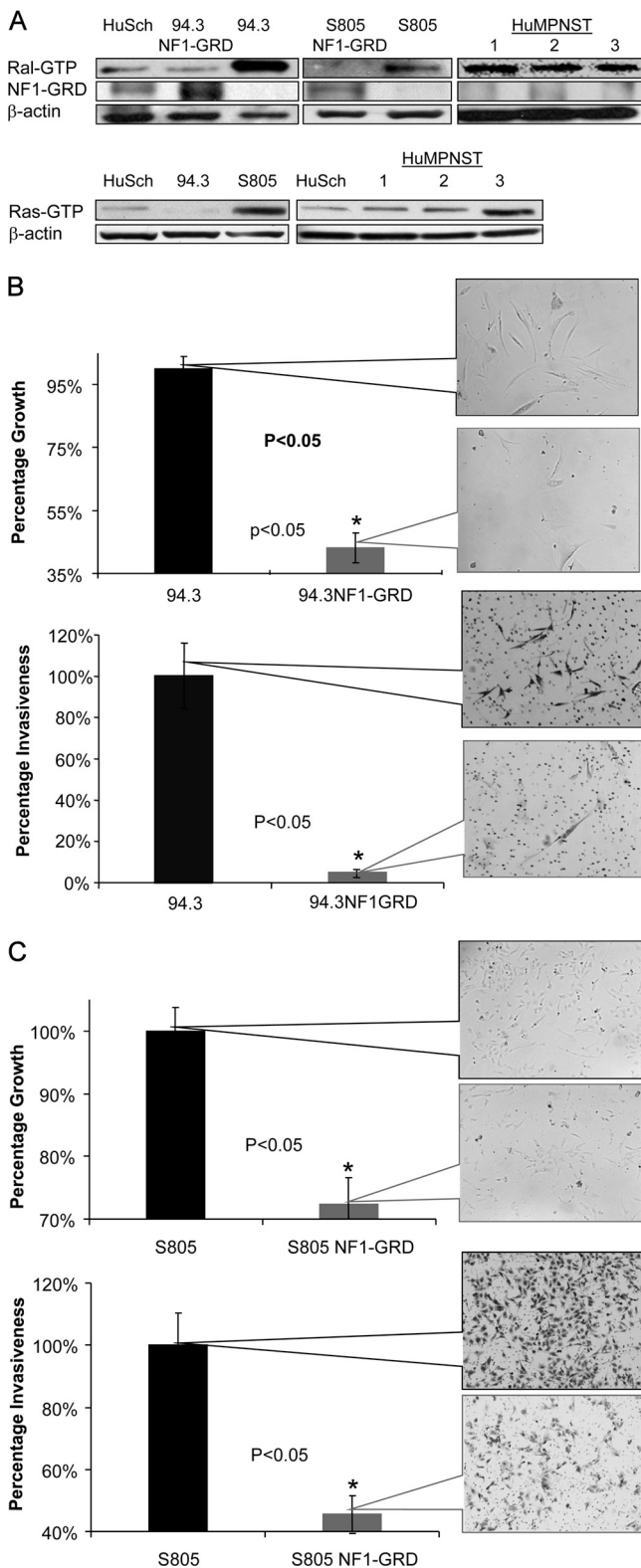


FIG. 4. Ral activation in human MPNST and Schwann cells and the effects of expression of NF1-GRD. (A) Ral activation was evaluated in lysates from two independent human MPNST cell lines (94.3 and S805), as well as three samples from human MPNST tumor tissues (HuMPNST-1, -2, and -3) and primary human nontransformed Schwann cells (HuSch). Although Ral-GTP levels were found to be elevated in 94.3 and S805 cells (compared to Schwann cells), such

Ral silencing reduces *in vivo* tumorigenicity of MPNST cells. Although the *in vitro* data mentioned above reveal many aspects of the role of Ral in the biology of MPNST cells, we focused on studying the impact of Ral silencing on the *in vivo* characteristics of these cells. For this purpose, 35-1-2 cells were electroporated with Ral-siRNA, sorted for cells containing siRNA and then injected s.c. into the left flank of severe combined immunodeficient (SCID-outbred) male mice (5×10^5 cells/flank, $n = 10$). An equal number of control-treated cells were injected into the right flank. Tumor sizes were measured every other day. As is seen in Fig. 6, Ral-silenced cells grew into smaller tumors at each time point postinjection ($P \leq 0.01$). Figure 6A shows the extent of tumor growth on two of the test subjects at days 10 and 16 postinjection (yellow circles focus on the sites of s.c. injections and tumoral masses). Figure 6B compares the tumor volumes (mean \pm the standard error) for the control and Ral-siRNA-treated sides. A significant retardation of the tumor growth was observed for the side injected with Ral-siRNA treated cells compared to control-treated cells.

In order to evaluate Ral activation, we extracted these s.c. tumors at 16 days postinoculation and evaluated Ral-GTP in lysates from these samples. Figure 6C shows three such tumors, their relative sizes, and the levels of Ral-GTP in each one of them. The overall size and Ral activation show notable reduction in the group treated with Ral-siRNA.

DISCUSSION

Ras signaling orchestrates highly complex molecular events that can, with aberrant activation, progress toward malignancy. In the last 20 years, the involvement of the Ral family of GTPases in human malignancies has been revealed, a fact originally not appreciated since the prominent role of Ral was not recognized in previously studied mouse models. Ral-GEF has since been found to be sufficient for Ras transformation in human cells (28), and Ral-GTP is understood to be chronically activated in cancer cell lines and tissues in comparison to their normal counterparts (12, 36, 37).

In NF-1, the loss of one copy of the neurofibromin tumor suppressor gene which encodes a Ras-GAP lowers the threshold for tumorigenesis while occurrence of a second hit is nec-

levels were reduced to amounts comparable to primary human non-transformed Schwann cells (or lower) upon transfection with NF1-GRD. Three human MPNST tumor tissue samples also show increased levels of Ral-GTP. In the lower panel, the activation of Ras was evaluated in 94.3 and S805 cells, along with lysates from three human MPNST tissue samples. S805 and HuMPNST-3 show prominent Ras overactivation compared to primary human nontransformed Schwann cells. (B) Expression of NF1-GRD reduces proliferation and invasiveness of 94.3 cells in a significant manner ($P < 0.05$). Callout panels represent the cell density at 48 h after infection of cells with the retrovirus expressing NF1-GRD or control retrovirus. The mean number of invaded cells for control groups is plotted as 100%, and the mean number of cells in NF1-GRD-treated group is plotted accordingly. (C) Proliferation and invasiveness of S805, another human MPNST primary cell, was reduced in a significant manner upon expression of NF1-GRD by a retrovirus. Callout panels represent cells at 48 h postinfection with NF1-GRD retrovirus.

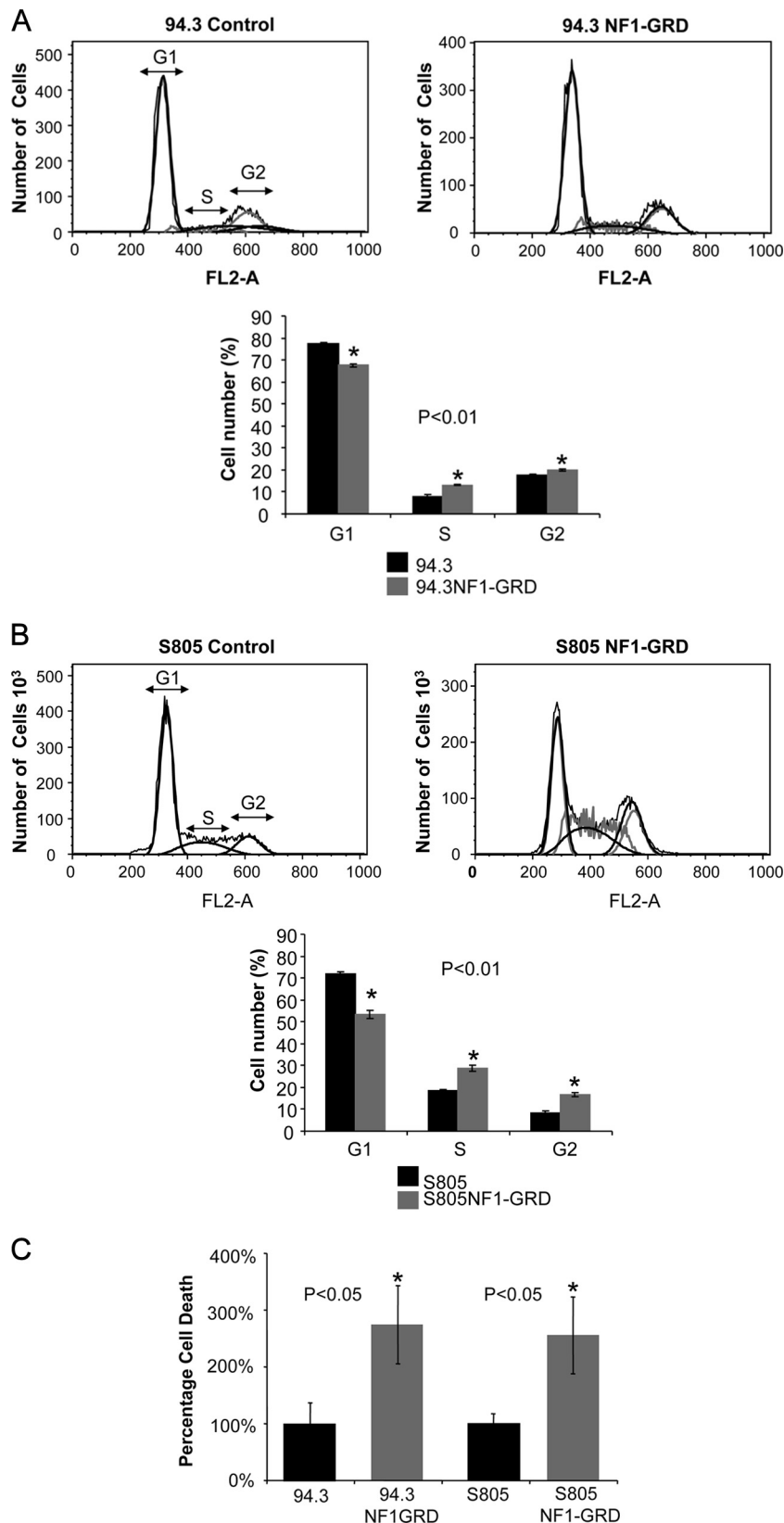


FIG. 5. Effects of expression of NF1-GRD on cell cycle progression and cell death in human MPNST cells. (A and B) Alterations in cell cycle progression upon expression of NF1-GRD in 94.3 and S805 human MPNST cells. Once NF1-GRD was expressed in these cells by exposure to a retrovirus for 48 h, a significant ($P < 0.01$) increase in the G_1 fraction was observed, along with an increase in cells in the S and G_2 phase. In the case of S805 cells, the same pattern of change was observed in terms of a decrease in the G_1 subpopulation. (C) The rate of cell death (apoptosis plus necrosis) was significantly increased ($P < 0.05$) upon exposure of human MPNST cells to the retrovirus expressing NF1-GRD compared to the control virus.

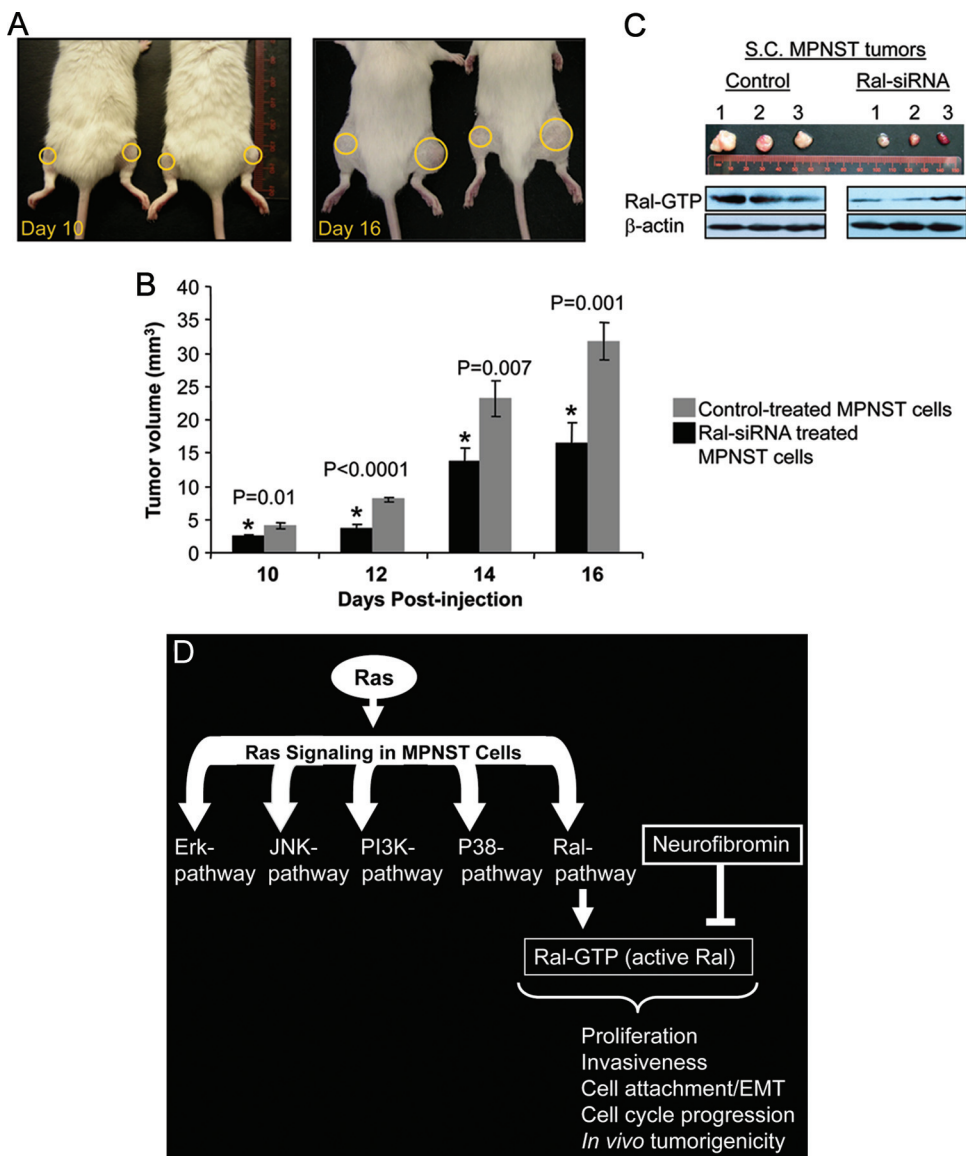


FIG. 6. Ral silencing reduces *in vivo* and *in vivo* tumorigenicity of MPNST cells and a model for involvement of Ral in the biology of MPNST. (A) SCID-Fox Chase outbred mice ($n = 10$) were injected s.c. with 5×10^5 Ral-siRNA (left flank) or control-treated cells (right flank). The panels represent the difference in tumor size at day 10 and day 16 postinjection. Yellow circles focus on the sites of injection and the tumoral mass. (B) Tumor volumes for Ral-siRNA and control-treated cells were measured and compared at each time point. A significant reduction in tumor size ($P \leq 0.01$) was observed in the Ral-siRNA treated group. (C) s.c. tumors were extracted at 16 days postinoculation, and the levels of Ral-GTP were evaluated in lysates from these samples. Three such tumors, their relative sizes, and the Ral-GTP amounts in each of them are shown in this panel. (D) Ras activation leads to the activation of a series of downstream effectors. Activation of Ral, which was observed in all mouse and human MPNST cells and tumor tissues, is involved in proliferation, invasion, cell attachment/EMT, cell cycle progression, and *in vivo* tumorigenesis. Neurofibromin deficiency promotes the activation of Ral as a Ras-independent mechanism evidenced by the reduced levels of Ral-GTP in cells expressing NF1-GRD.

essary for tumorigenesis. The subsequent deregulation in Ras-GAP activity has been assumed to cause an all-encompassing overactivation of Ras activity and its downstream signaling in neurofibromas (20, 29, 46). Our present work has examined this assumption by showing that mouse MPNST cells bearing deletions in both copies of the *Nf1* gene exhibit variations in their Ras-signaling portfolio. Only two of five different *Nf1*^{-/-}/*p53*^{-/-} MPNST cell lines expressed high levels of Ras-GTP, while the other three remained at levels comparable to nontransformed Schwann cells. These differences were also

found for the activity of Ras downstream signaling elements with the exception of Ral. Although the overall activation of ERK, JNK, p38 kinase, and PI3K pathways were higher in the MPNST cells with high levels of Ras-GTP, an elevated level of RalA activity was observed in all MPNST cells compared to untransformed Schwann cells. Therefore, the role of the Ral pathway in the development of MPNST and as a potential target for therapeutic strategies requires further study. Aside from *NF1* mutations, a series of genetic lesions, such as *p53* inactivation (39), *p16* inactivation (4), and *EGFR* overexpress-

sion (38), have been identified that cooperatively develop the background needed for formation of MPNSTs. In this platform, Ral overactivation can play a central role in linking such molecular abnormalities, considering the role of Ral in attenuation of p53-independent DNA damage response (1), involvement of p16 in blocking oncogenesis by RalGDS-related (Rgr) oncogene (43, 44), and the cooperation between Ral and EGFR in transforming cells (40). According to our data, gene-specific silencing for Ral, as well as reducing its activation via the expression of a dominant-negative Ral (S28N), can significantly impair the viability and invasiveness of MPNST cells, confirming the central role of Ral in supporting fundamental malignant characteristics of these cells. In addition, GGTI-2147 also reduced the viability of MPNST cells at concentrations which mainly reduced the active levels of Ral but not Ras. Untransformed Schwann cells, however, did not go through significant change in their viability upon Ral silencing, indicating a preferential dependence of transformed cells on this pathway. It is notable that although previous studies claimed that RalA had no effects on cell migration in bladder and prostate cancer cells (50), our studies in an MPNST model show that inhibition of RalA with different methods reduces invasiveness of these cells in a significant manner. However, differences in the molecular genetics of these cancers may be the primary reason for the observed differences in the role of RalA. The same reason might explain the observation by others that the depletion of RalA in the context of pancreatic cancer cells does not affect the viability of adherent cells (36). Further studies into the role of RalB in the biology of MPNST cells might also provide important information about the overall role of the Ral pathway in peripheral nerve sheath tumors.

Additional details about the effects of Ral silencing on invasion have been elucidated by our studies that assess the expression of EMT markers after Ral silencing. Changes in tumor tissue architecture allowing cancer cells to acquire invasive properties take place through EMT (31, 63). The important characteristics of EMT are the deregulation of intercellular contacts and increased cell mobility resulting in the release of cells from the parent epithelial tissue (26). Although the molecular bases of EMT is still being studied, several signal transduction pathways and a number of signaling molecules have been identified as involved. These include growth factors, receptor tyrosine kinases, Ras and other small GTPases, Src, β -catenin, and integrins (5, 63, 64). Recently, the role of the p38 kinase pathway in this process has also been identified as critical for downregulation of E-Cadherin (72). In addition, molecules such as ZO-1 and β -catenin, which shuttle between the plasma membrane and the nucleus or the cytosol, participate in the regulation of genes such as vimentin or matrix metalloproteinase-14, which are turned on during EMT (51). The effects of Ral silencing on EMT markers are for the most part antagonistic. In our study, we observed that the expression of two important transcription factors, β -catenin and Snail, is remarkably decreased. The expression of E-Cadherin (an anti-invasion molecule) is relatively unchanged, but the level of N-Cadherin (a proinvasion molecule) is decreased. Overall, this scenario shows that Ral overactivation is involved in enhancing the invasiveness of MPNST cells and driving the progression of EMT.

An important next step in our research was to shed light on

the potential mechanism for Ral activation in MPNST. To date, most of the focus in this field has been on the impact of lack of neurofibromin on Ras activation. Such central genetic abnormality, however, has not been investigated for its potential involvement in Ral activation, although some studies have suggested "Ras-independent" roles for neurofibromin via adenylyl cyclase (60) or focal adhesion kinase and mitogen-activated protein kinase (15). To investigate the role of Ral, we decided to express the GRD domain of NF1 in MPNST cells and evaluate the outcome of such a manipulation on active levels of Ral. We observed that in the case of both human MPNST cell lines, the levels of Ral-GTP were reduced upon NF1-GRD expression. Still unclear is whether neurofibromin has any direct GAP activity on Ral or if its effects are modulated via other modifiers of Ral activation such as Ral-GEFs, Aurora kinase A (61), or protein phosphatase 2A (PP2A $\alpha\beta$) (55). Once again, reduction in Ral activation by NF1-GRD was accompanied by reduction in the viability and invasiveness of 94.3 and S805 human MPNST cells. In addition, cell cycle progression in both cells was affected, with a decrease in G_1 and an increase in S and G_2 fractions.

Finally, we investigated whether Ral silencing would affect in vivo tumorigenicity of MPNST cells. Previous studies have shown different results in terms of involvement of RalA in SC tumor formation. RalA was found to be required for anchorage-independent growth in vitro and s.c. tumor growth in immunodeficient mice (36). However, inhibition of RalA did not affect tumor formation in metastatic prostate cancer cells but did abolish bone metastasis (71). Our data show the retardation of SC tumor growth of MPNST cells to a significant degree upon exposure to anti-RalA siRNA and the reduction of Ral levels in these tumors. Potential correlation between Ral activation and oncogene-induced senescence (16) is another possibility requiring further study in light of our data that show Ral overactivation in MPNST. The main question here is whether Ral activation in MPNST triggers negative feedback on Ral effectors and, if so, whether that process plays a role in the biology of benign neurofibromas.

In conclusion, our studies reveal that the activation of the Ral pathway (as shown for RalA) is consistently seen in mouse and human MPNST cells with important biological consequences on the characteristics of the malignant phenotype. Further research is required to explore in more detail the role of Ral activation in MPNST cells, including any potentially distinctive role for RalB, as well as possible strategies for intervening with Ral pathway that may have therapeutic benefits.

ACKNOWLEDGMENTS

This study was supported in part by Department of Defense-NF research program grant NF050014 to F.F.

We acknowledge the thoughtful advice and analysis by R. L. Martuza and S. D. Rabkin. We appreciate the editorial assistance of Michael J. Franklin, Martha Montello, and Amanda Wise.

REFERENCES

1. Agapova, L. S., J. L. Volodina, P. M. Chumakov, and B. P. Kopnin. 2004. Activation of Ras-Ral pathway attenuates p53-independent DNA damage G_2 checkpoint. *J. Biol. Chem.* **279**:36382–36389.
2. Aguirre-Ghiso, J. A., P. Frankel, E. F. Farias, Z. Lu, H. Jiang, A. Olsen, L. A. Feig, E. B. de Kier Joffe, and D. A. Foster. 1999. RalA requirement for v-Src- and v-Ras-induced tumorigenicity and overproduction of urokinase-type

- plasminogen activator: involvement of metalloproteases. *Oncogene* **18**:4718–4725.
3. Bajenaru, M. L., J. Donahoe, T. Corral, K. M. Reilly, S. Brophy, A. Pellicer, and D. H. Gutmann. 2001. Neurofibromatosis 1 (NF1) heterozygosity results in a cell-autonomous growth advantage for astrocytes. *Glia* **33**:314–323.
 4. Bajenaru, M. L., M. R. Hernandez, A. Perry, Y. Zhu, L. F. Parada, J. R. Garbow, and D. H. Gutmann. 2003. Optic nerve glioma in mice requires astrocyte Nf1 gene inactivation and Nf1 brain heterozygosity. *Cancer Res.* **63**:8573–8577.
 5. Baum, B., J. Settleman, and M. P. Quinlan. 2008. Transitions between epithelial and mesenchymal states in development and disease. *Semin. Cell Dev. Biol.* **19**:294–308.
 6. Bernot, D., A. M. Benoliel, F. Peiretti, S. Lopez, B. Bonardo, P. Bongrand, I. Juhan-Vague, and G. Nalbone. 2003. Effect of atorvastatin on adhesive phenotype of human endothelial cells activated by tumor necrosis factor alpha. *J. Cardiovasc. Pharmacol.* **41**:316–324.
 7. Bodemann, B. O., and M. A. White. 2008. Ral GTPases and cancer: linchpin support of the tumorigenic platform. *Nat. Rev. Cancer* **8**:133–140.
 8. Bollag, G., S. Freeman, J. F. Lyons, and L. E. Post. 2003. Raf pathway inhibitors in oncology. *Curr. Opin. Investig. Drugs* **4**:1436–1441.
 9. Brannan, C. L., A. S. Perkins, K. S. Vogel, N. Ratner, M. L. Nordlund, S. W. Reid, A. M. Buchberg, N. A. Jenkins, L. F. Parada, and N. G. Copeland. 1994. Targeted disruption of the neurofibromatosis type-1 gene leads to developmental abnormalities in heart and various neural crest-derived tissues. *Genes Dev.* **8**:1019–1029.
 10. Campbell, P. M., and C. J. Der. 2004. Oncogenic Ras and its role in tumor cell invasion and metastasis. *Semin. Cancer Biol.* **14**:105–114.
 11. Cantor, S. B., T. Urano, and L. A. Feig. 1995. Identification and characterization of Ral-binding protein 1, a potential downstream target of Ral GTPases. *Mol. Cell. Biol.* **15**:4578–4584.
 12. Chien, Y., and M. A. White. 2003. RAL GTPases are linchpin modulators of human tumour-cell proliferation and survival. *EMBO Rep.* **4**:800–806.
 13. Cichowski, K., and T. Jacks. 2001. NF1 tumor suppressor gene function: narrowing the GAP. *Cell* **104**:593–604.
 14. Cichowski, K., T. S. Shih, E. Schmitt, S. Santiago, K. Reilly, M. E. McLaughlin, R. T. Bronson, and T. Jacks. 1999. Mouse models of tumor development in neurofibromatosis type 1. *Science* **286**:2172–2176.
 15. Corral, T., M. Jimenez, I. Hernandez-Munoz, I. Perez de Castro, and A. Pellicer. 2003. NF1 modulates the effects of Ras oncogenes: evidence of other NF1 function besides its GAP activity. *J. Cell Physiol.* **197**:214–224.
 16. Courtois-Cox, S., S. M. Genter Williams, E. E. Reczek, B. W. Johnson, L. T. McGillicuddy, C. M. Johansson, P. E. Hollstein, M. MacCollin, and K. Cichowski. 2006. A negative feedback signaling network underlies oncogene-induced senescence. *Cancer Cell* **10**:459–472.
 17. Cox, A. D., and C. J. Der. 2002. Ras family signaling: therapeutic targeting. *Cancer Biol. Ther.* **1**:599–606.
 18. Downward, J. 2003. Targeting RAS signalling pathways in cancer therapy. *Nat. Rev. Cancer* **3**:11–22.
 19. Feig, L. A. 2003. Ral-GTPases: approaching their 15 minutes of fame. *Trends Cell Biol.* **13**:419–425.
 20. Feldkamp, M. M., L. Angelov, and A. Guha. 1999. Neurofibromatosis type 1 peripheral nerve tumors: aberrant activation of the Ras pathway. *Surg. Neurol.* **51**:211–218.
 21. Ferner, R. E. 2007. Neurofibromatosis 1. *Eur. J. Hum. Genet.* **15**:131–138.
 22. Frahm, S., A. Kurtz, L. Kluwe, F. Farassati, R. E. Friedrich, and V. F. Mautner. 2004. Sulindac derivatives inhibit cell growth and induce apoptosis in primary cells from malignant peripheral nerve sheath tumors of NF1-patients. *Cancer Cell Int.* **4**:4.
 23. Frankel, P., A. Aronheim, E. Kavanagh, M. S. Balda, K. Matter, T. D. Bunney, and C. J. Marshall. 2005. RalA interacts with ZONAB in a cell density-dependent manner and regulates its transcriptional activity. *EMBO J.* **24**:54–62.
 24. Giehl, K. 2005. Oncogenic Ras in tumour progression and metastasis. *Biol. Chem.* **386**:193–205.
 25. Goldfinger, L. E. 2008. Choose your own path: specificity in Ras GTPase signaling. *Mol. Biosyst.* **4**:293–299.
 26. Guarino, M., B. Rubino, and G. Ballabio. 2007. The role of epithelial-mesenchymal transition in cancer pathology. *Pathology* **39**:305–318.
 27. Gutmann, D. H. 2001. The neurofibromatoses: when less is more. *Hum. Mol. Genet.* **10**:747–755.
 28. Hamad, N. M., J. H. Elconin, A. E. Karnoub, W. Bai, J. N. Rich, R. T. Abraham, C. J. Der, and C. M. Counter. 2002. Distinct requirements for Ras oncogenesis in human versus mouse cells. *Genes Dev.* **16**:2045–2057.
 29. Harrisingh, M. C., and A. C. Lloyd. 2004. Ras/Raf/ERK signalling and NF1. *Cell Cycle* **3**:1255–1258.
 30. Harrisingh, M. C., E. Perez-Nadales, D. B. Parkinson, D. S. Malcolm, A. W. Mudge, and A. C. Lloyd. 2004. The Ras/Raf/ERK signalling pathway drives Schwann cell dedifferentiation. *EMBO J.* **23**:3061–3071.
 31. Hugo, H., M. L. Ackland, T. Blick, M. G. Lawrence, J. A. Clements, E. D. Williams, and E. W. Thompson. 2007. Epithelial-mesenchymal and mesenchymal-epithelial transitions in carcinoma progression. *J. Cell Physiol.* **213**:374–383.
 32. Jones, H. A., S. M. Hahn, E. Bernhard, and W. G. McKenna. 2001. Ras inhibitors and radiation therapy. *Semin. Radiat. Oncol.* **11**:328–337.
 33. Jullien-Flores, V., O. Dorseuil, F. Romero, F. Letourneur, S. Saragosti, R. Berger, A. Tavitian, G. Gacon, and J. H. Camonis. 1995. Bridging Ral GTPase to Rho pathways. RLP176, a Ral effector with CDC42/Rac GTPase-activating protein activity. *J. Biol. Chem.* **270**:22473–22477.
 34. Lakkis, M. M., and G. I. Tennekoon. 2000. Neurofibromatosis type 1. I. General overview. *J. Neurosci. Res.* **62**:755–763.
 35. Legius, E., H. Dierick, R. Wu, B. K. Hall, P. Marynen, J. J. Cassiman, and T. W. Glover. 1994. TP53 mutations are frequent in malignant NF1 tumors. *Genes Chromosomes Cancer* **10**:250–255.
 36. Lim, K. H., A. T. Baines, J. J. Fiordalisi, M. Shipitsin, L. A. Feig, A. D. Cox, C. J. Der, and C. M. Counter. 2005. Activation of RalA is critical for Ras-induced tumorigenesis of human cells. *Cancer Cell* **7**:533–545.
 37. Lim, K. H., K. O'Hayer, S. J. Adam, S. D. Kendall, P. M. Campbell, C. J. Der, and C. M. Counter. 2006. Divergent roles for RalA and RalB in malignant growth of human pancreatic carcinoma cells. *Curr. Biol.* **16**:2385–2394.
 38. Ling, B. C., J. Wu, S. J. Miller, K. R. Monk, R. Shamekh, T. A. Rizvi, G. Decourtner-Myers, K. S. Vogel, J. E. DeClue, and N. Ratner. 2005. Role for the epidermal growth factor receptor in neurofibromatosis-related peripheral nerve tumorigenesis. *Cancer Cell* **7**:65–75.
 39. Lothe, R. A., B. Smith-Sorensen, M. Heektoen, A. E. Stenwig, N. Mandahl, G. Saeter, and F. Mertens. 2001. Biallelic inactivation of TP53 rarely contributes to the development of malignant peripheral nerve sheath tumors. *Genes Chromosomes Cancer* **30**:202–206.
 40. Lu, Z., A. Hornia, T. Joseph, T. Sukezane, P. Frankel, M. Zhong, S. Bychenok, L. Xu, L. A. Feig, and D. A. Foster. 2000. Phospholipase D and RalA cooperate with the epidermal growth factor receptor to transform 3Y1 rat fibroblasts. *Mol. Cell. Biol.* **20**:462–467.
 41. Lundquist, E. A. 2006. Small GTPases. *WormBook* doi:10.1895/wormbook.1.67.1. www.wormbook.org.
 42. Lynch, T. M., and D. H. Gutmann. 2002. Neurofibromatosis 1. *Neurol. Clin.* **20**:841–865.
 43. Malumbres, M., I. Perez De Castro, M. I. Hernandez, M. Jimenez, T. Corral, and A. Pellicer. 2000. Cellular response to oncogenic *ras* involves induction of the Cdk4 and Cdk6 inhibitor p15^{INK4b}. *Mol. Cell. Biol.* **20**:2915–2925.
 44. Martello, L. A., and A. Pellicer. 2005. Biochemical and biological analyses of Rgr RalGEP oncogene. *Methods Enzymol.* **407**:115–128.
 45. Mashour, G. A., S. N. Drissel, S. Frahm, F. Farassati, R. L. Martuza, V. F. Mautner, A. Kindler-Rohrborn, and A. Kurtz. 2005. Differential modulation of malignant peripheral nerve sheath tumor growth by omega-3 and omega-6 fatty acids. *Oncogene* **24**:2367–2374.
 46. McCormick, F. 1995. Ras signaling and NF1. *Curr. Opin. Genet. Dev.* **5**:51–55.
 47. Menon, A. G., K. M. Anderson, V. M. Riccardi, R. Y. Chung, J. M. Whaley, D. W. Yandell, G. E. Farmer, R. N. Freiman, J. K. Lee, and F. P. Li. 1990. Chromosome 17p deletions and p53 gene mutations associated with the formation of malignant neurofibrosarcomas in von Recklinghausen neurofibromatosis. *Proc. Natl. Acad. Sci. USA* **87**:5435–5439.
 48. Moskalenko, S., D. O. Henry, C. Rosse, G. Mirey, J. H. Camonis, and M. A. White. 2002. The exocyst is a Ral effector complex. *Nat. Cell Biol.* **4**:66–72.
 49. Mousley, C. J., K. R. Tyeryar, M. M. Ryan, and V. A. Bankaitis. 2006. Sec14p-like proteins regulate phosphoinositide homeostasis and intracellular protein and lipid trafficking in yeast. *Biochem. Soc. Trans.* **34**:346–350.
 50. Oxford, G., C. R. Owens, B. J. Titus, T. L. Foreman, M. C. Herlevsen, S. C. Smith, and D. Theodorescu. 2005. RalA and RalB: antagonistic relatives in cancer cell migration. *Cancer Res.* **65**:7111–7120.
 51. Polette, M., M. Mestdagt, S. Bindels, B. Nawrocki-Raby, W. Hunziker, J. M. Foidart, P. Birembaut, and C. Gilles. 2007. Beta-catenin and ZO-1: shuttle molecules involved in tumor invasion-associated epithelial-mesenchymal transition processes. *Cells Tissues Organs* **185**:61–65.
 52. Rajalingam, K., R. Schreck, U. R. Rapp, and S. Albert. 2007. Ras oncogenes and their downstream targets. *Biochim. Biophys. Acta* **1773**:1177–1195.
 53. Rasmussen, S. A., and J. M. Friedman. 2000. NF1 gene and neurofibromatosis 1. *Am. J. Epidemiol.* **151**:33–40.
 54. Rey, J. A., A. Pestana, and M. J. Bello. 1992. Cytogenetics and molecular genetics of nervous system tumors. *Oncol. Res.* **4**:321–331.
 55. Sablina, A. A., W. Chen, J. D. Arroyo, L. Corral, M. Hector, S. E. Bulmer, J. A. DeCaprio, and W. C. Hahn. 2007. The tumor suppressor PP2A A β regulates the RalA GTPase. *Cell* **129**:969–982.
 56. Serra, E., S. Puig, D. Otero, A. Gaona, H. Krueyer, E. Ars, X. Estivill, and C. Lazarou. 1997. Confirmation of a double-hit model for the NF1 gene in benign neurofibromas. *Am. J. Hum. Genet.* **61**:512–519.
 57. Sherman, L. S., R. Atit, T. Rosenbaum, A. D. Cox, and N. Ratner. 2000. Single cell Ras-GTP analysis reveals altered Ras activity in a subpopulation of neurofibroma Schwann cells but not fibroblasts. *J. Biol. Chem.* **275**:30740–30745.
 58. Sugihara, K., S. Asano, K. Tanaka, A. Iwamatsu, K. Okawa, and Y. Ohta. 2002. The exocyst complex binds the small GTPase RalA to mediate filopodia formation. *Nat. Cell Biol.* **4**:73–78.
 59. Thomas, S. L., G. D. Deadwyler, J. Tang, E. B. Stubbs, Jr., D. Muir, K. K.

- Hiatt, D. W. Clapp, and G. H. De Vries. 2006. Reconstitution of the NF1 GAP-related domain in NF1-deficient human Schwann cells. *Biochem. Biophys. Res. Commun.* **348**:971–980.
60. Tong, J., F. Hannan, Y. Zhu, A. Bernardis, and Y. Zhong. 2002. Neurofibromin regulates G protein-stimulated adenylyl cyclase activity. *Nat. Neurosci.* **5**:95–96.
61. Tong, T., Y. Zhong, J. Kong, L. Dong, Y. Song, M. Fu, Z. Liu, M. Wang, L. Guo, S. Lu, M. Wu, and Q. Zhan. 2004. Overexpression of Aurora-A contributes to malignant development of human esophageal squamous cell carcinoma. *Clin. Cancer Res.* **10**:7304–7310.
62. Trovo-Marqui, A. B., and E. H. Tajara. 2006. Neurofibromin: a general outlook. *Clin. Genet.* **70**:1–13.
63. Tse, J. C., and R. Kalluri. 2007. Mechanisms of metastasis: epithelial-to-mesenchymal transition and contribution of tumor microenvironment. *J. Cell Biochem.* **101**:816–829.
64. Turley, E. A., M. Veiseh, D. C. Radisky, and M. J. Bissell. 2008. Mechanisms of disease: epithelial-mesenchymal transition—does cellular plasticity fuel neoplastic progression? *Nat. Clin. Pract. Oncol.* **5**:280–290.
65. Upadhyaya, M., G. Spurlock, E. Majounie, S. Griffiths, N. Forrester, M. Baser, S. M. Huson, D. G. Evans, and R. Ferner. 2006. The heterogeneous nature of germline mutations in NF1 patients with malignant peripheral nerve sheath tumours (MPNSTs). *Hum. Mutat.* **27**:716.
66. van Dam, E. M., and P. J. Robinson. 2006. Ral: mediator of membrane trafficking. *Int. J. Biochem. Cell Biol.* **38**:1841–1847.
67. Vasudevan, A., Y. Qian, A. Vogt, M. A. Blaskovich, J. Ohkanda, S. M. Sebti, and A. D. Hamilton. 1999. Potent, highly selective, and non-thiol inhibitors of protein geranylgeranyltransferase-I. *J. Med. Chem.* **42**:1333–1340.
68. Vogel, K. S., L. J. Klesse, S. Velasco-Miguel, K. Meyers, E. J. Rushing, and L. F. Parada. 1999. Mouse tumor model for neurofibromatosis type 1. *Science* **286**:2176–2179.
69. Weiss, B., G. Bollag, and K. Shannon. 1999. Hyperactive Ras as a therapeutic target in neurofibromatosis type 1. *Am. J. Med. Genet.* **89**:14–22.
70. Yamamoto, T., S. Taya, and K. Kaibuchi. 1999. Ras-induced transformation and signaling pathway. *J. Biochem.* **126**:799–803.
71. Yin, J., C. Pollock, K. Tracy, M. Chock, P. Martin, M. Oberst, and K. Kelly. 2007. Activation of the RalGEF/Ral pathway promotes prostate cancer metastasis to bone. *Mol. Cell. Biol.* **27**:7538–7550.
72. Zohn, I. E., Y. Li, E. Y. Skolnik, K. V. Anderson, J. Han, and L. Niswander. 2006. p38 and a p38-interacting protein are critical for downregulation of E-cadherin during mouse gastrulation. *Cell* **125**:957–969.